Midrapidity Hyperon Production in pp and pA Collisions from Low to LHC Energies

G.H. ARAKELYAN, C. MERINO, and Yu.M. SHABELSKI.
Departamento de Física de Partículas & Instituto Galego de Física de Altas Enerxías
Universidade de Santiago de Compostela, 15782 Santiago de Compostela, Galiza, Spain
carlos.merino@usc.es

QUARK MATTER 2015
The XXVth International Conference on Ultrarelativistic Nucleus-Nucleus Collisions

arXiv:1509.05218[hep-ph]

The experimental data on p, Λ, Ξ^-, Ω^--baryons and the corresponding antibaryons spectra obtained by different collaborations are compared with the results of the calculations performed into the frame of the Quark-Gluon String Model.

The contribution of String Junction diffusion and the inelastic screening corrections are accounted for in the theoretical calculations.

The predictions of the Quark-Gluon String Model both for pp and pA collisions are extended up to the LHC energies.

In QGSM, the inclusive spectrum of a secondary hadron is determined by the convolution of the diquark, valence quark, and sea quark distributions in the incident particles with the fragmentation function of quarks and diquarks into the secondary hadron.

String Junction contribution

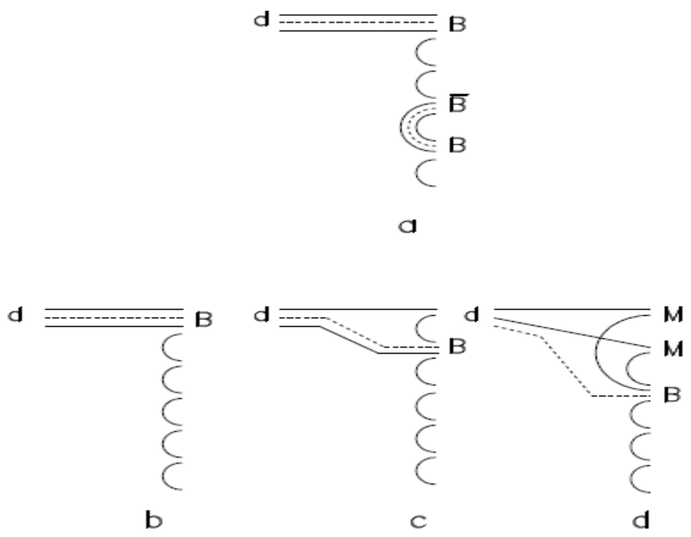

Figure 2: QGSM diagrams describing secondary baryon production: (a) usual $B\overline{B}$ central production with production of new SF pair; (b) initial SF together with two valence quarks and one sea quark; (c) initial SF together with one valence quark and two sea quarks; (d) initial SF together with three sea quarks.

Interactions with neclei at high energies and inelastic screening effects

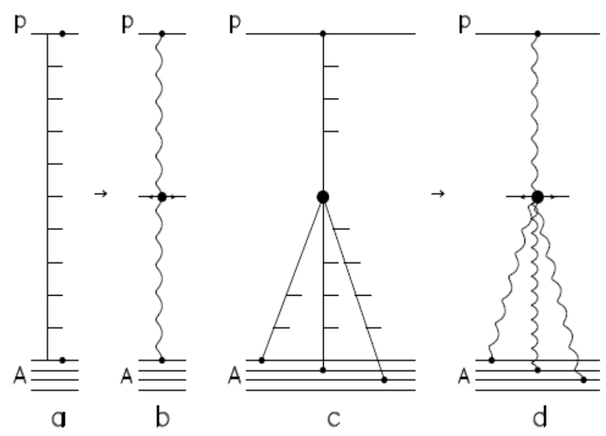

Figure 3: One of the diagrams for the inelastic interaction of one incident proton with two target nucleons N_1 and N_2 in a pA collision.

The pp collisions

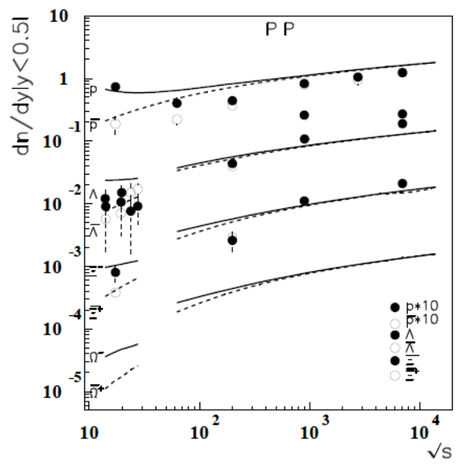

Figure 5: The energy dependence of baryon and antibaryon production inclusive densities $dn/dy(|\ y\ | \leq 0.5)$ in the midrapidity region in pp collisions (baryons are shown by closed points and full curves, and antibaryons by open points and dashed curves).

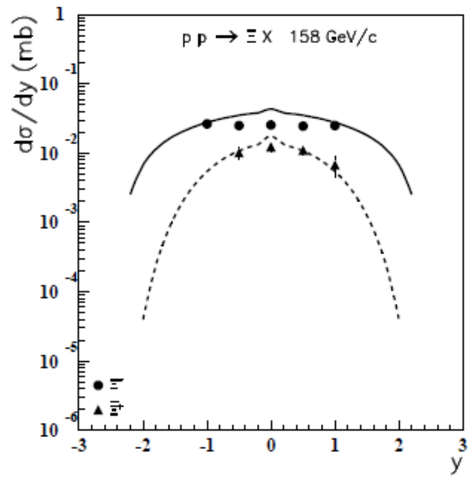

Figure 7: The QGSM results for the rapidity dependence of the inclusive cross section $d\sigma/dy$ of Ξ^- and $\overline{\Xi}^+$ productions in pp collisions at 158 GeV/c, and their comparison with the experimental data [54]. The full curve corresponds to Ξ^- and the dashed curve to $\overline{\Xi}^+$ production.

The pA collisions

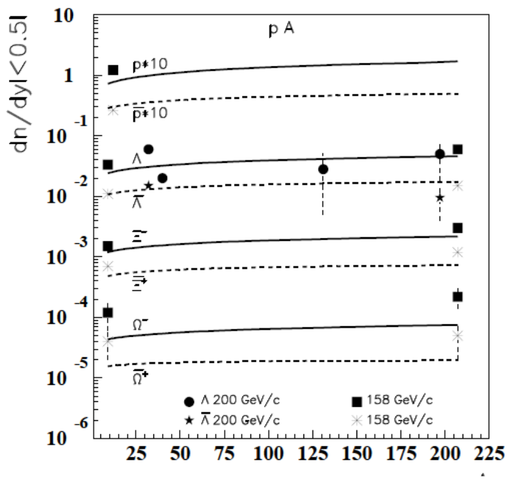

Figure 9: Comparison of experimental data on the A-dependence of midrapidity denstity dn/dy ($|\ y\ | \leq 0.5$) of p, $\overline{p}$, and Λ, $\overline{\Lambda}$, Ξ^-, $\overline{\Xi}^+$, Ω^-, and $\overline{\Omega}^+$ hyperons produced at 158 Gev/c and 200 GeV/c [71, 73, 74, 75], with the results of corresponding QGSM calculations

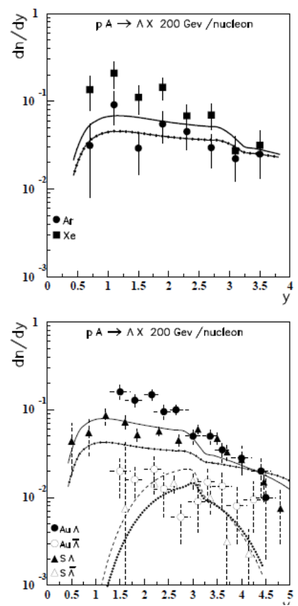

Figure 12: The experimental data on the rapidity dependence of the production denstities of Λ hyperon produced in proton collisions on Ar and Xe nuclei [73] (upper panel) and of Λ and $\overline{\Lambda}$ hyperons produced in proton collisions on S and Au nuclei [74, 75, 76] (lower panel), all at 200 GeV/c, together with the results of the corresponding QGSM calculations

The QGSM, based on the Dual Topological Unitarization, Regge phenomenology and nonperturbative notions of QCD, provides a reasonable description of strange and multistrange hyperons production, as well as of the production of their corresponding antiparticles, both in pp and pA collisions for a wide range of energies, by including into the analysis the contribution of String Junction diffusion and the inelastic screening corrections.

It is important to note that in the QGSM the extension of the calculations of the hyperon (antihyperon) productions from pp collisions to proton-nucleus collisions does not require any additional model parameters. The accuracy of our calculations can be estimated to be on the level of ~15%.

Experimental References

[52] G. Aad *et al.*, ATLAS Collaboration, Phys. Rev. **D85**, 012001 (2012).
[53] V. Khachatryan *et al.*, CMS Collaboration, JHEP 1105 (2011) 064; arXiv:1102.4282[hep-ex].
[54] D. Barna, NA49 Collaboration, PhD Thesis, 2002.
[55] J.W. Chapman *et al.*, Phys. Lett **B47**, 465 (1975).
[56] D. Brick *et al.*, Nucl. Phys. **B164**, 1 (1980).
[57] F. Lopinto *et al.*, Phys. Rev. **D22**, 323 (1980).
[58] K. Jaeger *et al.*, Phys. Rev. **D11**, 2405 (1975).
[59] A. Sheng *et al.*, Phys. Rev. **D11**, 722 (1975).
[60] H. Kichimi *et al.*, Phys. Rev. **D20**, 37 (1979) and arXiv:1111.1297[hep-ex].
[61] B. Abelev *et al.*, STAR Collaboration, Phys. Rev.**C75**, 064901 (2007) and arXiv:nucl-ex/06007033.
[62] M.Aguilar-Benitez *et al.*, Z. Phys. **C50** (1991) 405
[63] A. Adare *et al.*, PHENIX Collaboration, Phys. Rev. **C83**, 064903 (2011).
[64] B. Abelev *et al.*, STAR Collaboration, Phys. Rev. **C79**, 034909 (2009)
[65] S. Chatrchyan *et al.*, CMS Collaboration, Eur. Phys. J. **C72**, 2164 (2012).
[66] K. Aamodt *et al.*, ALICE Collaboration, Eur. Phys. J. **C71**, 1655 (2011).
[67] J.K. Adam *et al.*, ALICE Collaboration, arXiv:1504.00024[nucl-ex].
[71] F. Antinori *et al.*, NA57 Collaboration, J. Phys. **G32**,427 (2006) and arXiv:0601021[nucl-ex].
[72] B. Baatar *et al.*, NA49 Collaboration, Eur. Phys. J. **C73**, 2364 (2013).
[73] E. Derado *et al.*, NA5 Collaboration, Z. Phys. **C50**, 31 (1991).
[74] A. Bamberger *et al.*, NA35 Collaboration, Z. Phys. **C41**, 25 (1989).
[75] J. Bartke *et al.*, NA35 Collaboration, Z. Phys. **C48**, 191 (1990).
[76] T. Alber *et al.*, NA35 Collaboration, Z. Phys. **C64**, 195 (1994).

G.H. Arakelyan (A.Alikhanyan National Scientific Institute-Yerevan Physics Institute, Armenia)
Yu.M. Shabelski (Petersburg Nuclear Physics Institute-NCR Kurchatov Institute, Russia)

This paper was supported by Ministerio de Ciencia e Innovación of Spain under project FPA2014-58293-C2-1-P, the Spanish Consolider-Ingenio 2010 Programme CPAN (CSD2007-00042), by Xunta de Galicia, Spain (2011/PC043), and, in part, by Russian grant RSGSS-3628.2008.2 and by State Committee of Science of the Republic of Armenia, Grant-13-1C023.-00281.